Volume 27
Number 17
August 24, 1988

Inorganic Chemistry

Communications

Photoluminescence and Electrogenerated Chemiluminescence of Palladium(0) and Platinum(0) Complexes of Dibenzylideneacetone and Tribenzylideneacetylacetone

Sir:

We wish to report here the first examples of electrogenerated chemiluminescence (ECL) for d^{10} transition metal (TM) complex systems and of room temperature photoluminescence for organometallic Pd(0) and Pt(0) complexes.[1] The compounds involved are bimetallic and trimetallic species of the general formula $M_2(dba)_3$ and $M_3(tbaa)_3$, respectively (where M = Pd(0) or Pt(0), dba = dibenzylideneacetone, and tbaa = tribenzylideneacetylacetone). A novel structural feature of all these complexes is that metal–ligand bonding is wholly metal–olefin in type. Prior X-ray structural determinations on both the chloroform[2] and dichloromethane[3] solvates of $Pd_2(dba)_3$ reveal that each Pd is trigonally coordinated to an olefin group of each of the three bridging dibenzylideneacetone ligands, with a short nonbonding Pd–Pd separation of 3.24 Å. Detailed ^1H NMR studies on a range of deuteriated derivatives of $Pd_2(dba)_3$[4] and the analogous $Pt_2(dba)_3$ complex[5] have established that a trigonal molecular structure for each species is maintained in solution. Spectroscopic investigations on the related trimetallic $Pd_3(tbaa)_3$[6] and $Pt_3(tbaa)_3$[7] species also indicate a trigonal geometry about the metal with each of the three C=C bonds of one tbaa ligand coordinated to each of the three metal atoms. All the compounds are unusually air-stable in room-temperature solution, and several studies have described the versatility of these species as reagents for ligand-exchange and oxidative-addition reactions.[6-9] However, no literature information is available on their photophysical and photochemical properties, despite an increasing interest in such studies on d^{10} Pd(0) and Pt(0) systems.[10,11]

The electronic absorption spectra for the four complexes and the free ligands are presented in Table I. The intense purplish color of the bimetallic and trimetallic compounds is atypical of Pd(0) and Pt(0) and is suggestive of some metal–metal interaction. For example, the corresponding monometallic species, $M(dba)_3$, are known[12,13] and do not exhibit an absorption band at lower energy than that of the intraligand $n \rightarrow \pi^*$ transition at approximately 320 nm. The extent of metal–metal and metal–ligand interactions must be very similar for the $M_2(dba)_3$ and $M_3(tbaa)_3$ systems, based on the very close correspondence of the electronic absorption spectra of $Pd_2(dba)_3$ and $Pd_3(tbaa)_3$, and likewise of $Pt_2(dba)_3$ and $Pt_3(tbaa)_3$ (Table I). Recently, Ito et al.[14] concluded from a cyclic voltammetric (CV) and spectroscopic study of a variety of substituted dba species that the LUMO in the $M_2(dba)_3$ complexes was delocalized over a π-framework composed of the metal and three phenylolefin moieties. We thus assign the lowest

Table I. Absorption and Emission Properties of $M_2(dba)_3$, $M_3(tbaa)_3$, and Related Species

	absorption[a]		emission 295 K[a]			emission 77 K[b]	
species	λ_{max}, nm	ϵ	λ_{max}, nm	τ, μs	Φ_{em}[c]	λ_{max}, nm	τ, μs
dba[d]	325	2.4×10^4					
tbaa	327	2.4×10^4					
$Pd_2(dba)_3$	327	6.2×10^4	726	≤0.1	0.29	740	8.3
	529	1.3×10^4					
$Pd_3(tbaa)_3$	327	4.5×10^4	724	≤0.1	0.28	740	8.3
	529	1.2×10^4					
$Pt_2(dba)_3$	320	4.9×10^4	782	≤0.1	0.95	795	0.87
	567	9.5×10^3					
$Pt_3(tbaa)_3$	320	6.1×10^4	782	≤0.1	1.05	810	0.87
	570	1.6×10^4					

[a] CH_2Cl_2 solution. [b] 2:1 ether/ethanol glass. [c] Φ_{em} = relative emission quantum yields on 436-nm excitation versus $[Cr(bpy)_3](ClO_4)_3$.[17] [d] Reference 11.

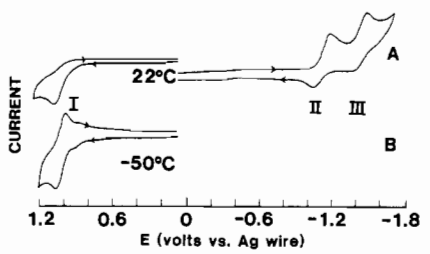

Figure 1. Cyclic voltammogram of a 1.2×10^{-4} M $Pt_3(tbaa)_3/CH_2Cl_2/0.1$ M TBAP solution at a Pt electrode (scan rate 100 mV/s, Ag wire quasi-reference electrode): (A) at 22 °C, (B) at −50 °C. Under our conditions a value of 0.24 V was obtained at 22 °C for the ferrocenium ion/ferrocene reduction poential.[19]

(1) Lees, A. J. *Chem. Rev.* **1987**, *87*, 711.
(2) Ukai, T.; Kawazura, H.; Ishii, Y.; Bonnett, J. J.; Ibers, J. A. *J. Organomet. Chem.* **1974**, *65*, 253.
(3) Mazza, M. C.; Pierpont, C. G. *J. Chem. Soc., Chem. Commun.* **1973**, 207; *Inorg. Chem.* **1974**, *13*, 1891.
(4) Kawazura, H.; Tanaka, H.; Yamada, K.; Takahashi, T.; Ishii, Y. *Bull. Chem. Soc. Jpn.* **1978**, *51*, 3466.
(5) Tanaka, H.; Kawazura, H. *Bull. Chem. Soc. Jpn.* **1979**, *52*, 2815.
(6) Ishii, Y.; Hasegawa, S.; Kimura, S.; Itoh, K. *J. Organomet. Chem.* **1974**, *73*, 411.
(7) Stackhouse, G. B., IV; Comalander, D. R.; Crosby, T. E.; Tweet, W. S.; Konkel, K.; Wright, L. L., submitted for publication in *Organometallics*.
(8) Moseley, K.; Maitlis, P. M. *J. Chem. Soc., Dalton Trans.* **1974**, 169.
(9) Ito, T.; Hasegawa, S.; Takahashi, Y.; Ishii, Y. *J. Organomet. Chem.* **1974**, *73*, 401.
(10) Caspar, J. V. *J. Am. Chem. Soc.* **1985**, *107*, 6718.
(11) Harvey, P. D.; Schaefer, W. P.; Gray, H. B. *Inorg. Chem.* **1988**, *27*, 1101; Harvey, P. D.; Gray, H. B. *J. Am. Chem. Soc.* **1988**, *110*, 2145.
(12) Moseley, K.; Maitlis, P. M. *J. Chem. Soc., Chem. Commun.* **1971**, 982.
(13) Mazza, M. C.; Pierpont, C. G. *Inorg. Chem.* **1973**, *12*, 2955.
(14) Ito, N.; Tetsuo, S.; Shigeru, A. *J. Electroanal. Chem. Interfacial Electrochem.* **1983**, *144*, 153.

0020-1669/88/1327-2905$01.50/0

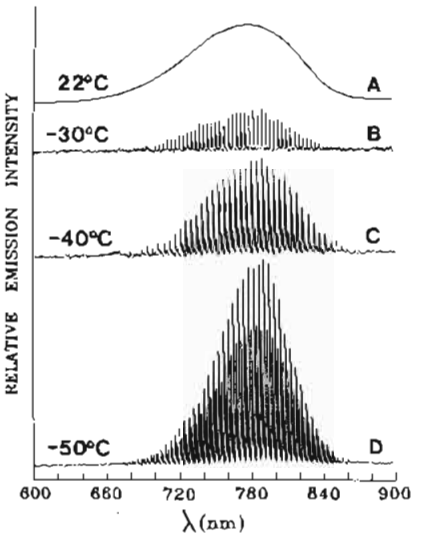

Figure 2. (A) Photoluminescence spectrum of a 7.8×10^{-5} M $Pt_3(tbaa)_3$ solution in CH_2Cl_2 on 436-nm excitation (22 °C). (B–D) ECL spectra at low temperatures of a 1.2×10^{-4} M $Pt_3(tbaa)_3/CH_2Cl_2/0.1$ M TBAP solution (pulsing limits +1.2 and −1.9 V vs Ag quasi-reference electrode at 1 Hz; Au working electrode, Pt auxiliary electrode).

energy absorption band for the $M_2(dba)_3$ and $M_3(tbaa)_3$ systems as predominantly d(metal) → π^* in character.

All four complexes exhibit relatively strong photoluminescence in room-temperature solution upon excitation into their first two absorption bands (Table I and Figure 2A).[15] Strong evidence against impurities as the source of this emission is provided by the correspondence between the excitation spectra of the emission and the corresponding absorption spectra of the complexes. Comparable room-temperature emission intensities were obtained in CH_2Cl_2, $CHCl_3$, $CDCl_3$, acetone, ether, and toluene solutions. The emission signals were unaffected by dissolved oxygen or a 10:1 molar excess of free ligand and remained effectively constant for several hours if solutions were stored in the dark. The relative emission quantum yields at 22 °C for 436-nm absorbance-matched CH_2Cl_2 solutions were substantially greater for the Pt(0) systems (Table I), with that observed for $Pt_2(dba)_3$ and $Pt_3(tbaa)_3$ being 95% and 105%, respectively, of that obtained for an absorbance-matched air-saturated aqueous solution of $[Cr(bpy)_3](ClO_4)_3$.[17] Although emission lifetimes were short in room-temperature solution (≤100 ns), when the solution was cooled to 77 K (2:1 ether/ethanol glass), a dramatic enhancement in intensities and lifetimes was detected, accompanied by a small red shift in the emission maximum (Table I). The higher energy of the Pd(0) versus Pt(0) complex emission maxima is in accord with the relative energies of their long-wavelength absorption bands, and we tentatively assign the emission as $\pi^* \rightarrow$ d charge transfer (probably triplet → singlet). These observations are of special significance since the number of d^{10} Pd(0) and Pt(0) complexes known to exhibit solution luminescence is very small, being restricted to several trigonal[10,11] and tetrahedral[11] phosphine systems recently described by Caspar[10] and Gray and co-workers.[11]

In view of their relatively strong photoluminescence, we have also examined these compounds as candidates for ECL—a phenomenon as yet unreported for d^{10} TM complex systems (and very rare for organometallic systems in general).[1] In the prior CV studies on the $Pd_2(dba)_3$ and $Pt_2(dba)_3$ species by Ito et al.,[14] two reversible one-electron-reduction steps and an irreversible one-electron-oxidation step were reported. We find the tbaa systems behave very similarly, and a typical CV for $Pt_3(tbaa)_3$ in $CH_2Cl_2/0.1$ M tetrabutylammonium perchlorate (TBAP) solution is shown in Figure 1A. For all four complexes the free energy difference between the oxidation wave in region I and the reduction wave in region II (Figure 1) is approximately 2.2 V—a value significantly in excess of the spectroscopic energy of the emissive state (approximately 1.7 eV and 1.6 eV for the Pd(0) and Pt(0) systems, respectively). Thus, if the applied potential is pulsed between cathodic and anodic limits that are sufficient to produce the reduced (P^-) and the oxidized (P^+) forms of the parent species (P), then the subsequent thermal back-electron-transfer reaction is sufficiently exergonic for one of the parent molecules to be regenerated in its luminescent excited state; i.e., ECL generation may be possible via a radical anion/cation annihilation pathway such as shown in reaction 1.[20]

$$P^- + P^+ \rightarrow P + {}^*P \rightarrow \text{ECL} \qquad (1)$$

No ECL is in fact observed for room-temperature solutions of the four complexes when the working electrode (Pt or Au) is stepped between +1.2 and −1.3 V (or −1.9 V). However, for $Pt_3(tbaa)_3$, strong ECL is detected from Pt or Au working electrodes when pulse limits of +1.2 and −1.9 V are employed and the cell temperature is lowered to −50 °C (Figure 2D). Comparable results are observed for $Pt_2(dba)_3$ under the same experimental conditions, while no ECL signal is observed in the absence of complex. For both Pt(0) compounds the anodic voltage required for the onset of ECL (approximately 1.0 V) matches closely that associated with the onset of the anodic wave observed in region I of their cyclic voltammograms (Figure 1). The intensity of the ECL is also dependent on the cathodic limit potential employed for the working electrode. Intense ECL signals are only generated on stepping this voltage to values more negative than or equal to that for the second reduction wave of the complex (region III, Figure 1).

The ECL spectra for both $Pt_3(tbaa)_3$ and $Pt_2(dba)_3$ match closely the corresponding photoluminescence spectra (Figure 2A). The marked ECL temperature dependence may be attributed in part to the longer emissive excited state lifetimes at lower temperatures (Table I). However, this fact alone would not readily account for the exceedingly weak ECL signal of the analogous Pd(0) systems at −50 °C. The limiting factor for these latter species appears to be the irreversibility of their redox couple in region I even at low temperature, while the corresponding couple for the two Pt(0) compounds exhibit some reversibility at −50 °C (Figure 1). These observations argue for a longer lived P^+ species in the Pt(0) cases and thus for a stronger ECL signal via a redox pathway similar to reaction 1. This conclusion receives dramatic support from the ECL spectra in Figure 2B–D. At −30 °C, ECL is only observed when the working electrode is stepped to the anodic pulse limit (consistent with a short P^+ lifetime), while at lower temperatures an ECL signal also becomes increasingly evident at the cathodic pulse limit. These results suggest that cell temperature be employed as an important variable in investigations of possible ECL from other TM complex systems.

Further studies on the ECL behavior and photochemical properties of these and related Pd(0) and Pt(0) complexes are in progress and will be reported elsewhere.

Acknowledgment. The support of this research by the donors of the Petroleum Research Fund, administered by the American Chemical Society (L.L.W.), and the Camille and Henry Dreyfus

(15) Uncorrected photoluminescence and ECL spectra were recorded by using instrumentation and procedures described previously.[16] Excitation spectra were obtained on a Spex Fluorolog-2 (Model F111A). Excited-state lifetimes (Table II) were determined by using the 355-nm frequency tripled line of a Nd:YAG Laser (Spectra Physics, Model DCR-11) for excitation and a Nicolet 4094 digital oscilloscope with Model 4175 plug-in for signal detection and analysis.

(16) Kane-Maguire, N. A. P.; Guckert, J. A.; O'Neill, P. J. *Inorg. Chem.* **1987**, *26*, 2340.

(17) The emission maxima for the Pd(0) complexes are essentially identical to that for $[Cr(bpy)_3](ClO_4)_3$ (727 nm), for which Kirk and Porter report a phosphoresence quantum yield of 8.9×10^{-4} in air-saturated aqueous solution at 20 °C.[18] At the 782-nm emission maximum for the Pt(0) systems, manufacturer data for the R446S detector suggest a spectral response of approximately half that at 727-nm.

(18) Kirk, A. D.; Porter, G. B. *J. Phys. Chem.* **1980**, *84*, 887.

(19) Gagne, R. R.; Koval, C. A.; Lisensky, G. C. *Inorg. Chem.* **1980**, *19*, 2854.

(20) Tokel-Takvoryan, N. E.; Hemingway, R. E.; Bard, A. J. *J. Am. Chem. Soc.* **1973**, *95*, 6582 and references therein.

Foundation (N.A.P.K.-M.) is gratefully acknowledged. We also gratefully acknowledge the support of the Duke Endowment and the assistance of Drs. John Petersen and Kevin Goodwin of Clemson University in obtaining excitation spectra.

Department of Chemistry
Furman University
Greenville, South Carolina 29613

N. A. P. Kane-Maguire*
L. L. Wright*
J. A. Guckert
W. S. Tweet

Received April 19, 1988

Remarkably Diverse Interstitial Chemistry of the Polar Intermetallic Phase Zr_5Sb_3

Sir:

We have found that the hexagonal phase Zr_5Sb_3 exhibits a rich interstitial chemistry in which any one of at least 18 different elements (Z) with a wide variety of normal valence requirements can be bonded in the center of octahedral Zr_6Sb_6 units therein. An essential feature of this structure (Mn_5Si_3 type) is the presence of chains of confacial trigonal antiprismatic ("octahedral") Zr_6 units sheathed by antimony (Figure 1).

In the past, a number of compounds with the Mn_5Si_3 structure have been surmised or shown to bond heteroatoms in the octahedral sites within the chain or, in some cases, even to *require* the third atom for stability,[1,2] oxygen or carbon in the Zr_5Sb_3 case, for example.[3] Similar Zr_5Sb_3Z phases with Z = Ni, Cu, or Zn have also been reported,[4] although this seems chemically counterintuitive alongside the oxygen example. However, these phases were all prepared by sintering elemental mixtures in evacuated fused-silica containers at 800 °C for up to 8 weeks, a procedure that raises questions about both possible contamination by the container and inadequate equilibration at this relatively low temperature. Furthermore, products were identified only by comparison of lattice constants plus intensities of calculated vs observed X-ray powder diffractometer data, and we have found similar changes in both can be mimicked by other products, those of the binary Zr_5Sb_{3+x}, for example.[5]

Suitable synthetic techniques have now been refined so that distinctive samples that are *single phase* by Guinier powder diffraction can be regularly produced. Arc melting of the samples under argon followed by annealing, sintering of the powdered mixtures at ~1100 °C, or vapor phase transport utilizing ZrI_4 near 1300 °C have all been utilized, generally in Ta containers. These techniques were first applied to the identification of the ten intermediate phases in the Zr–Sb binary system and, in particular, to establish that the binary Zr_5Sb_3 does exist in the Mn_5Si_3 structure.[6] In fact, a nonstoichiometric Zr_5Sb_{3+x} with self-interstitials over the range $0 \leq x \leq 0.4$ is present according to a single-crystal structural study coupled with variations in the Guinier-based lattice constants as a function of composition. A second, nonrelevant structure of the Y_5Bi_3 type is obtained at high temperatures.[5]

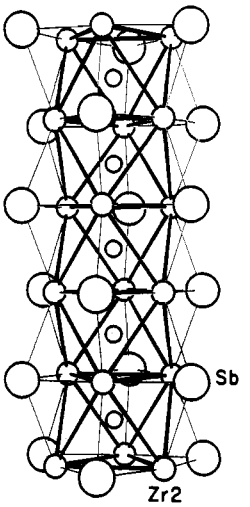

Figure 1. Portion of a confacial Zr_6Sb_6 octahedral chain in Zr_5Sb_3: large circles, Sb; midsized circles, Zr; small circles, interstitial site.

The variety of interstitials Z that may be individually incorporated in the Zr_5Sb_3 host is chemically astounding. Those established to date sort out in a periodic array as follows:

						C		O
					Al	Si	P	S
Fe	Co	Ni	Cu	Zn	Ga	Ge	As	Se
Ru			Ag				Sb	

Especially noteworthy is the occurrence of all the elements in the fourth period from iron through selenium. On the other hand, the lighter alkali and alkaline-earth metals have yielded only negative results while Cr and Mn are problematical. A majority of the ternary phases have been identified on the basis of shifts in Guinier-based lattice parameters observed for sintered or vapor-phase-transported samples. The lattice constant variations, which have earlier been used as the diagnosis for compound formation, are neither particularly large (≤4% over the whole range) nor informative about the relative dimensional changes within the Zr_6Z units. A few of the phases appear to be non- or substoichiometric (Fe, Co, Ni, S, Sb).

Most importantly, the location and occupancy of the interstitial in the Zr_5Sb_3Z phases have been established by seven single-crystal X-ray studies for Z = Fe, Zn, Si, $S_{0.7}$, Al (where some site interchange with Sb apparently occurs), a mixed $Fe_{2/3}In_{1/3}$ system, and the self-interstitial $Sb_{0.16}$. (Data for the iron and sulfur examples are given in the supplementary material.) These appear to be the first single-crystal studies reported on any phases in this general structure class beyond those involving self-interstitials that are in the fully occupied limit known as the Ti_5Ga_4-type structure.[3] A recent Rietveld refinement of high-temperature X-ray powder data has also delineated the $Zr_5Al_3O_{0.3}$ analogue.[7]

This series of structures provides some useful generalizations. The dimensional changes seen in the structures on incorporation of the seven Z examples are largely limited to a 0.22-Å range in the shared edges of the trigonal antiprisms that lie normal to the chain (Figure 1). In contrast, Zr–Sb distances remain quite uniform throughout, while the limited (0.09 Å) expansion along the chain may be viewed as a restriction imposed by the presence of a second, linear, parallel and tightly bound zirconium chain in the structure with a $c/2$ repeat (not shown).

Extended Hückel band calculations on Zr_5Sb_3 and its sulfur and iron derivatives provide some enlightenment about the bonding and electronic distributions. As might be anticipated for such a polar host, the empty cluster exhibits a broad valence band that lies well below the Fermi level E_F. This contains all antimony 5p states plus appreciable contributions from 4d orbitals on both types of zirconium required for covalency in the bonding. A broad conduction band above about −1.5 eV contains only zirconium

(1) Rossteutscher, W.; Schubert, K. *Z. Metallkd.* **1965**, *56*, 813.
(2) Nowotny, H.; Benesovsky, F. In *Phase Stability in Metals and Alloys*; Rudman, P. S., Stringer, J., Jaffee, R. I., Eds.; McGraw-Hill: New York, 1966; p 319.
(3) Pearson, W. B. *The Crystal Chemistry and Physics of Metals and Alloys*; Wiley-Interscience: New York, 1972; pp 718, 720.
(4) Rieger, W.; Parthé, E. *Acta Crystallogr., Sect. B: Struct. Crystallogr. Cryst. Chem.* **1968**, *B24*, 456.
(5) Garcia, E.; Corbett, J. D. *Inorg. Chem.* **1988**, *27*, 2353.
(6) Garcia, E.; Corbett, J. D. *J. Solid State Chem.* **1988**, *74*, 440, 452.
(7) Kim, S.-J.; Kematick, R. J.; Yi, S. S.; Franzen, H. F. *J. Less-Common Met.* **1988**, *137*, 55.

0020-1669/88/1327-2907$01.50/0